J. Appl. Phys. **78**,2362 (1996).

Atomistic Models of Vacancy-Mediated Diffusion in Silicon

Scott T. Dunham and Can Dong Wu
Department of Electrical, Computer and Systems Engineering,
Boston University, Boston, MA 02215

Abstract

Vacancy-mediated diffusion of dopants in silicon is investigated using Monte-Carlo simulations of hopping diffusion, as well as analytic approximations based on atomistic considerations. Dopant/vacancy interaction potentials are assumed to extend out to third-nearest neighbor distances, as required for pair diffusion theories. Analysis focusing on the third-nearest neighbor sites as bridging configurations for uncorrelated hops leads to an improved analytic model for vacancy-mediated dopant diffusion. The Monte-Carlo simulations of vacancy motion on a doped silicon lattice verify the analytic results for moderate doping levels. For very high doping ($> 2 \times 10^{20}\text{cm}^{-3}$) the simulations show a very rapid increase in pair diffusivity due to interactions of vacancies with more than one dopant atom. This behavior has previously been observed experimentally for group IV and V atoms in silicon [Nylandsted Larsen *et al.*, *J. Appl. Phys.* **73**, 691 (1993)], and the simulations predict both the point of onset and doping dependence of the experimentally-observed diffusivity enhancement.

1 Introduction

The diffusion of dopant atoms in silicon takes place via interactions with point defects, interstitials and vacancies [1]. Consideration of the atomistic basis of these processes leads to greater insight into diffusion processes, while providing, as in this work, the basis for understanding deviations from the simple theory. In this paper, we analyze the interactions of dopants with vacancies and find that the assumptions inherent in pair diffusion models lead to greatly enhanced dopant diffusion at very high doping concentrations. This phenomena has been observed experimentally for vacancy diffusers in silicon (Sb, As, Ge, Sn) [2], but is not typically included in process simulation. We begin by developing analytic models for vacancy-mediated diffusion in silicon at moderate doping levels. We use full three-dimensional Monte-Carlo simulations of vacancy hopping diffusion on the doped silicon (diamond) lattice to verify the analytic models and extend the analysis to very high doping levels, where interactions of vacancies with multiple dopants can be expected.

2 Modeling of Vacancy-Mediated Diffusion

The observation that dopant diffusivity is much more rapid than silicon self-diffusion leads to the conclusion that there exists an attractive potential between dopants and defects that results in the formation of dopant/defect pairs, whereby the defect takes part in many hops of the same dopant before dissociating [3]. These pair diffusion theories provide the basis for our current understanding of diffusion in silicon [1, 4, 5]. Consideration of the mobile species as dopant/defect pairs is fully consistent for interstitial-mediated diffusion, as long as the concept of a pair is generalized to include an interstitial dopant atom (which has both dopant and interstitial attributes). However, for vacancy-mediated diffusion, there is a fundamental complication in that during the movement of a dopant onto a vacant site, the vacancy moves in the opposite direction. Subsequent displacements of the dopant by the same vacancy simply result in the dopant and vacancy re-exchanging places, without any net displacement of the dopant. Due to the silicon lattice structure, the vacancy must move away to at least a third-nearest neighbor site in order to return along a different path (Fig. 1). Thus, the diffusing pair must partially dissociate and reform many times before finally fully dissociating, with the third-nearest neighbor sites playing a critical role as bridging configurations.

To investigate the diffusion process, we begin by noting that the fundamental process leading to diffusive behavior is the hopping of an atom from one site to another. Diffusivity due to hopping diffusion can be written as [6]

$$D = \alpha^2 \nu_{\text{eff}}/6, \tag{1}$$

where $\alpha = \sqrt{3}a/4$ is the jump distance (a is the size of the cubic cell) and $\nu_{\text{eff}} = f \sum \nu_j$ is the effective mean hopping rate if each dopant hop was uncorrelated to previous hops (f is the correlation factor and the ν_j are the rates of possible hops). For self-diffusion via vacancies on a diamond lattice, the correlation factor is 0.5 [7] and there are four nearest neighbors. Thus $\nu_{\text{eff}} = 2\nu_V^0 (C_V^0/C_S)$, so

$$D = \alpha^2 \nu_V^0 (C_V^0/C_S)/3, \tag{2}$$

where ν_V^0 is the hopping rate for vacancies and (C_V^0/C_S) is the fraction of lattice sites occupied by vacancies, with the superscript 0 in both cases indicating values for vacancies far away from any dopant atoms.

Due to the attractive potential between dopants and vacancies, there are many vacancies located on the sites adjacent to dopants, which results in a correspondingly large number of dopant hops. However, when there is a strong first-nearest neighbor attraction, dopants and vacancies primarily just exchange places over and over, with no long range migration. Thus, for vacancy-mediated dopant diffusion, the effective hopping rate is much smaller than the actual rate of dopant displacement (equivalent to $f \ll 1$).

Focusing on the pivotal role of the third-nearest neighbor sites, we recognize that the critical rate is how often vacancies move from third to second-nearest neighbor sites, since as long as the attractive potential between dopants and vacancies decreases with distance, these vacancies are highly likely to exchange sites with the dopant atom before separating to a third-nearest neighbor distance again. Thus, the effective hopping rate is proportional to the fraction of dopants with vacancies at third-nearest neighbor sites and the rate of hopping of those vacancies to second-nearest neighbor sites:

$$\nu_{\text{eff}} = \frac{1}{2} \left[C_{DV}^{3\text{nn}}/C_D \right] (2f\nu_{32}), \tag{3}$$

where $C_{DV}^{3\text{nn}}$ is the number of third-nearest neighbor pairs and ν_{32} is the rate of hopping from third to second-nearest neighbor positions. The initial factor of one-half in Equation (3) accounts for the fact that half of the time the vacancy will end up exiting by its initial path after an even number of dopant/vacancy exchanges, but no net dopant displacement. The factor of two in the second term accounts for the two possible second-nearest neighbor sites adjacent to each third-nearest neighbor. The correlation factor is given by [6]

$$f = \frac{1 + \langle \cos\theta \rangle}{1 - \langle \cos\theta \rangle} \tag{4}$$

where $\langle \cos\theta \rangle$ is the average projection of hop direction on that of the previous hop. For diffusion via the third-nearest neighbor bridging sites, there are two possible directions, one of which is a reversal of the previous hop ($\cos\theta = -1$) and the other has $\cos\theta = 1/3$ ($\theta = 70.6°$), so $\langle \cos\theta \rangle = (-1 + 1/3)/2 = -1/3$ and $f = 0.5$.

In order to calculate the dopant diffusivity based on Equation (3), we must specify the dopant/vacancy interaction potential as shown in Figure 2. Since it is necessary to account for pair diffusion behavior, we consider a dopant/defect interaction out to third-nearest neighbor distances, with binding energies at first, second and third-nearest neighbor distances (ΔE_1, ΔE_2, ΔE_3). Given the binding energies, the number of third-nearest neighbor pairs is

$$C_{DV}^{3\mathrm{nn}} = 12 \left(\frac{C_V^0}{C_s} \right) \exp\left(\frac{\Delta E_3}{kT} \right), \tag{5}$$

where the factor of 12 accounts for the number of third-nearest neighbor sites.

To estimate hopping rates, we assume that the entropy of migration is the same as for vacancies far away from any dopant atoms, but that the migration barrier is altered due to the dopant/vacancy attraction. To estimate the migration barrier, we assume that the vacancy energy in the transition state is given by the sum of the barrier for vacancies far away from dopant atoms (ΔE_m) and the average of the vacancy energy in the two adjoining sites (Fig. 2). Thus the rate of hopping from third to second-nearest neighbor sites is

$$\nu_{32} = \left[\nu_V^0 \exp\left(\frac{\Delta E_2 - \Delta E_3}{2kT} \right) \right], \tag{6}$$

where the change in migration energy from the free vacancy is just one-half of the change in energy between the final and initial states.

Substituting Equations (5) and (6) in Equation (1),

$$D = \alpha^2 \left(\frac{C_V^0}{C_s} \right) \nu_V^0 \exp\left(\frac{\Delta E_2 + \Delta E_3}{2kT} \right). \tag{7}$$

Note that this expression differs from the work of Hu [5] in accurately specifying the pre-exponential term and replacing ΔE_3 with $(\Delta E_2 + \Delta E_3)/2$ in the activation energy. The difference in the activation energy reflects the change in the migration energy associated with the role of the transition state between the second and third-nearest neighbor sites as the peak barrier for pair diffusion. Hu's analysis neglected the reduction in the migration barrier associated with the changes in binding energy between sites, but the effect was included in the numerical results. Thus Equation (7) results in an improved match to Hu's numerical results (activation energy of $0.57E_b$, compared to Hu's numerical value of $0.58E_b$ and predicted value of $0.52E_b$).

3 Very Heavily-Doped Material

Nylandsted Larsen *et al.* [2] measured the diffusivity of group IV and V elements (As, Ge, Sb, Sn) in silicon doped with high background levels of phosphorus and found that dopant diffusivity increases very sharply at doping levels above about $2 \times 10^{20}\text{cm}^{-3}$. In the previous section, we assumed that the doping density was low enough that each vacancy interacts with at most one dopant atom. However, at such high doping levels, a vacancy is likely to interact with more than one dopant at a time. For example, a vacancy on a third-nearest neighbor site to one dopant is also likely to have another dopant atom within an interaction distance, with the attractive potential due to the second dopant atom reducing the energy for a vacancy located on that site as illustrated in Figure 3. The net result is to reduce the activation energy for pair diffusion associated with third to second-nearest neighbor transitions, thereby increasing the dopant diffusivity. This behavior has previously been considered by Mathiot and Pfister [8, 9], who invoked a percolation phenomena to describe the resulting diffusivity enhancement.

To estimate the effect of interactions of vacancies with multiple dopant atoms within the framework described above, ν_{eff} becomes a weighted average of rates over all possible dopant configurations in the neighborhood of a vacancy. Since the probability of having n dopants within an interaction distance of a vacancy is proportional to $(C_D/C_s)^n$, the diffusivity can be expected to have a polynomial form:

$$D = D^{\text{int}}\left[1 + \beta_1\left(\frac{C_D}{C_s}\right) + \beta_2\left(\frac{C_D}{C_s}\right)^2 + \ldots\right], \tag{8}$$

where D^{int} (Equation (7)) is the diffusivity in moderately-doped material. The β_i depend on sums over configurations involving interactions of vacancies with $i+1$ dopant atoms. These values could potentially be calculated, but the large number of possible configurations and the inapplicability of the simplifying assumptions used in deriving Equation (7) make the problem much more difficult.

4 Lattice Monte-Carlo Simulations

In order to test the analytic model, as well as to consider the more complicated interactions present at very high doping levels, we conducted a series of atomistic Monte-Carlo simulations of vacancy movement on a doped silicon lattice. The simulations were conducted using periodic boundary conditions on an $N_x \times N_y \times N_z$ array of cubic cells, each with 8 lattice sites.

To initialize the system, dopant atoms are placed at random on the lattice sites according to the designated doping density. Next, vacancies are placed on lattice sites with the probability of occupation based on the binding energy for each site as calculated by determining the number of dopants in the neighborhood:

$$p_V = \frac{p_V^0}{1 + \exp\left(\dfrac{\Delta E}{kT}\right)} \tag{9}$$

where p_V^0 is the probability of occupation for sites far from any dopant atoms. The binding energies are assumed additive:

$$\Delta E = -(n_1 \Delta E_1 + n_2 \Delta E_2 + n_3 \Delta E_3), \tag{10}$$

where n_i represents the number of dopant atoms on i^{th}-nearest neighbor sites.

The simulations proceed through the movement of vacancies on the lattice, with dopant diffusion resulting when dopants are displaced. To account for the interaction potential between the vacancies and dopants, the vacancy hopping rates are biased by changes in system energy associated with prospective hop:

$$\nu = \nu_V^0 \exp\left(\frac{\Delta E_f - \Delta E_i}{2kT}\right), \tag{11}$$

where ΔE_f and ΔE_i are the final and initial system energies, respectively. The main contribution to changes in the system energy generally comes from the changing neighborhood of the hopping vacancy; however, when dopants are displaced, the energies of other vacancies in the neighborhood change as well.

At any point in time, there are $4 \times N_V$ possible vacancy hops (corresponding to the four directions possible for each vacancy), each with associated rates ν_j^i. At each time step, a hop is chosen at random weighted by these hopping rates. Because any hop which results in the displacement of a dopant changes the hopping rates for other nearby dopants, hops are considered in a serial fashion. After each hop, the vacancy and dopant distributions are updated, and rates are recalculated within the neighborhood of the hop. Assuming Poisson processes, the expected time before the next vacancy hop is given by

$$\Delta t = \left[\sum_{i=1}^{N_V} \sum_{j=1}^{4} \nu_j^i\right]^{-1}. \tag{12}$$

Therefore, the time is incremented by this amount for each hop. This process is continued until a specified time or number of hops has elapsed. Typical runs use on the order of 10^7 hops in a system containing at least 200 dopants and 200 vacancies. The system size varies strongly with dopant density, ranging from about 10^4 to 10^7 lattice sites. In order to determine the dopant diffusivity, the mean squared displacement of dopant atoms over the course of the simulation is calculated to give [6]

$$D = \langle |\Delta \vec{x}|^2 \rangle / 6t. \tag{13}$$

The displacement is also checked periodically throughout each run in order to ensure that the diffusivity remains approximately constant as the system evolves. We have observed some fluctuations in diffusivity after long times, which may be associated with the formation of clusters due to the effective dopant/dopant binding which is a secondary byproduct of the dopant/vacancy attraction. However, all results shown are for shorter times, for which the diffusivity is uniform.

5 Simulation Results

The parameters for the system are the dopant/vacancy binding energies as a function of displacement. For the first-nearest neighbor binding energies, we used the experimental lower bounds for arsenic (1.23 eV) or phosphorus (1.04 eV) from Hirata *et al.* [10]. Since no data is available for the second and third-nearest neighbor binding energies, we simply used 2/3 and 1/3 of the nearest neighbor energy, respectively. Equation (7) also depends on the equilibrium concentration and hopping rate for vacancies far away from any dopants, but we eliminate these terms by normalizing our results to the tracer self-diffusion coefficient due to vacancies (Equation (2)). The majority of the simulations used a bulk vacancy occupation probability of 10^{-6}, corresponding to an equilibrium concentration of $5 \times 10^{16}\mathrm{cm}^{-3}$. Higher vacancy densities resulted in improved statistics, but above this level the simulated diffusivity began to saturate, instead of varying linearly with vacancy density as observed at lower densities.

As initial tests of the Monte-Carlo simulations, as well as the analytic derivations, we compared results for both tracer self-diffusion (all binding energies zero) and dopant diffusivity at moderate doping levels ($< 10^{20}\mathrm{cm}^{-3}$). In both cases, we found good agreement between theory and simulation. Examples of the comparison for dopant diffusivity are included in Figure 4.

Figure 4 illustrates how dopant diffusivity as obtained from the lattice Monte-Carlo simulations varies as a function of doping level. In agreement with the analysis in Sections 2 and 3, the normalized diffusivity is nearly uniform at low and moderate doping levels and then rises rapidly for doping levels above about $1.5 \times 10^{20}\mathrm{cm}^{-3}$, manifesting an approximate third or fourth power dependence on the doping level. Note that the dopant diffusivity is normalized by the tracer self-diffusion coefficient (Equation (2)), which removes the dependence on changes in vacancy concentration due to Fermi level shifts. Thus the remaining variation in diffusivity with doping level are due to reduction in the migration energy of the dopant/vacancy pair associated with interactions of vacancies with multiple dopants.

Previous modeling of vacancy-mediated diffusion at very high doping levels has invoked a percolation phenomena [8, 9], which leads to an initial abrupt rise in the diffusivity when the doping exceeds the percolation threshold, followed by more gradual increases at higher doping levels (negative curvature for $\log(D)$ versus $\log(C_D)$) [2, 9]. However, no such behavior appears in our simulations or in the experimental observations [2], both of which are more consistent with the polynomial behavior expected based on our analysis. The problem with using a percolation model for the system considered in this work stems from the fact that we are not looking at the diffusion of vacancies, which may display percolation behavior as transfer between dopant atoms becomes easy at very high doping levels, but rather dopant diffusion, for which the reduction in energy for migration of a dopant/defect pair is the critical factor.

The results of the simulations agree well with the experimental observations of Nylandsted Larsen *et al.* [2], with a good match to both the doping level at which the onset of enhanced pair diffusion is observed ($\sim 2 \times 10^{20}\mathrm{cm}^{-3}$) and the dependence of diffusivity with increasing concentration. If we assume that the dopant diffuses via singly-charged vacancies (as is standard for arsenic in n-type material [11, 12]), we can add in the changes in vacancy density due to Fermi level effects:

$$D = D^{-}\left(\frac{C_D}{n_i}\right)\left[1 + \left(\frac{C_D}{C^{*}}\right)^{n}\right], \tag{14}$$

where D^{-} is the dopant diffusivity due to negatively-charged vacancies in intrinsic material, C^{*} is based on the simulation results as shown in Figure 4, and we assume that the dopant is fully activated with $C_D \gg n_i$. The resulting fourth or fifth power dependence of diffusivity on doping level at very high concentrations matches the power dependence of between 3 and 5 observed by Nylandsted Larsen *et al.* for arsenic, antimony, tin and germanium.

The simulation predictions can also be compared directly to the experimental results [2]. Since the experiments used high phosphorus background doping, the enhancement in arsenic diffusivity at very high doping levels results primarily from the effect of phosphorus atoms on the diffusion of the arsenic/vacancy pairs. Thus, in order to predict how the diffusivity is expected to change with doping level, we ran a series of simulations using the phosphorus/vacancy binding energy [10] to derive a value for C^* ($3 \times 10^{20}\mathrm{cm}^{-3}$ at 1050°C for $n = 4$). We combined this value with D^- as calculated from the measured diffusivity at moderate doping levels ($< 1.5 \times 10^{20}\mathrm{cm}^{-3}$) and compared the result to the experimental measurements for arsenic as illustrated in Figure 5. This comparison shows that the simulations do a good job of predicting how dopant diffusivity changes with doping level at very high doping levels.

6 Conclusions

In summary, we have developed an atomistic theory for dopant diffusion via vacancy interactions and validated the predictions of that theory using lattice Monte-Carlo simulations. The analysis provides a correction to previous work of Hu [5] at moderate doping levels and confirms the central role of third-nearest neighbor interactions. Both analysis and simulation show that full consideration of the assumptions inherent in pair diffusion models requires that the effective pair diffusivity will increase at very high doping concentrations, with an approximately polynomial dependence on the doping density. The simulations show a dependence of diffusivity on doping level that is consistent with experimental measurements for vacancy diffusers in silicon (Sb, As, Ge and Sn) [2].

When compared directly to experimental results for arsenic diffusion in high phosphorus backgrounds, the simulations accurately predict how diffusivity changes with concentration at very high doping levels. They show good agreement with the doping level at which interactions of vacancies with multiple dopants start to increase diffusivity ($\sim 2 \times 10^{20}\mathrm{cm}^{-3}$), as well as the subsequent dependence of diffusivity on doping ($\propto C_D^n$ with $4 < n < 5$ for diffusion via negatively-charged vacancies).

7 Acknowledgments

This work was supported by NSF and SRC/SEMATECH.

References

[1] P. M. Fahey, P. B. Griffin and J. D. Plummer, *Rev. Mod. Phys.* **61**, 289 (1989).

[2] A. Nylandsted Larsen, K. Kyllesbech Larsen, P. E. Andersen, B. G. Svensson, *J. Appl. Phys.* **73**, 691 (1993).

[3] R. P. Johnson, *Phys. Rev.* **56**, 814 (1939).

[4] S. M. Hu, *Phys. Rev.* **180**, 773 (1969).

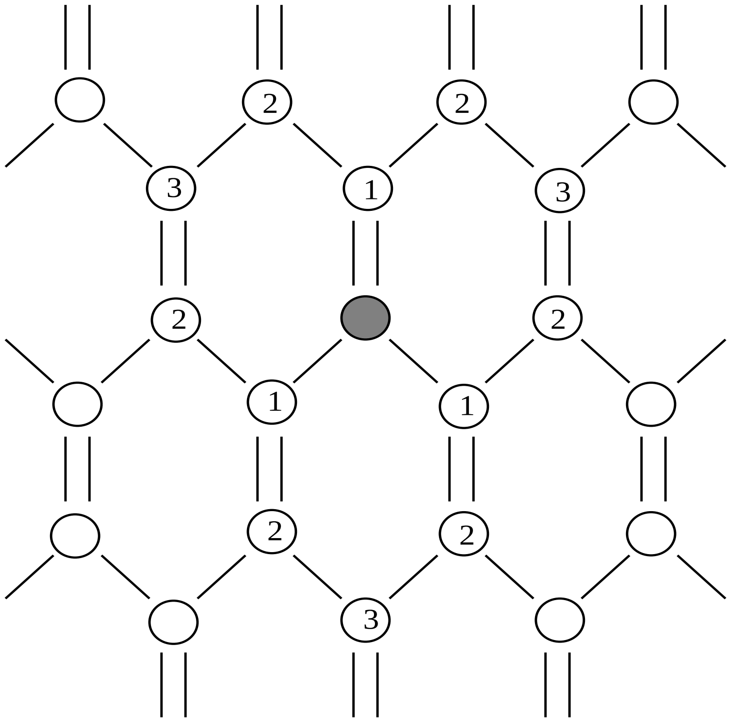

Figure 1: Schematic of silicon lattice structure as viewed in $\langle 110 \rangle$ direction, with sites labeled with distance from the dopant atom (filled). Double lines connecting atoms indicate bonds angled into and out of the plane of the figure. Note that it is necessary for a vacancy to move out to a third-nearest neighbor site in order to return along a different path.

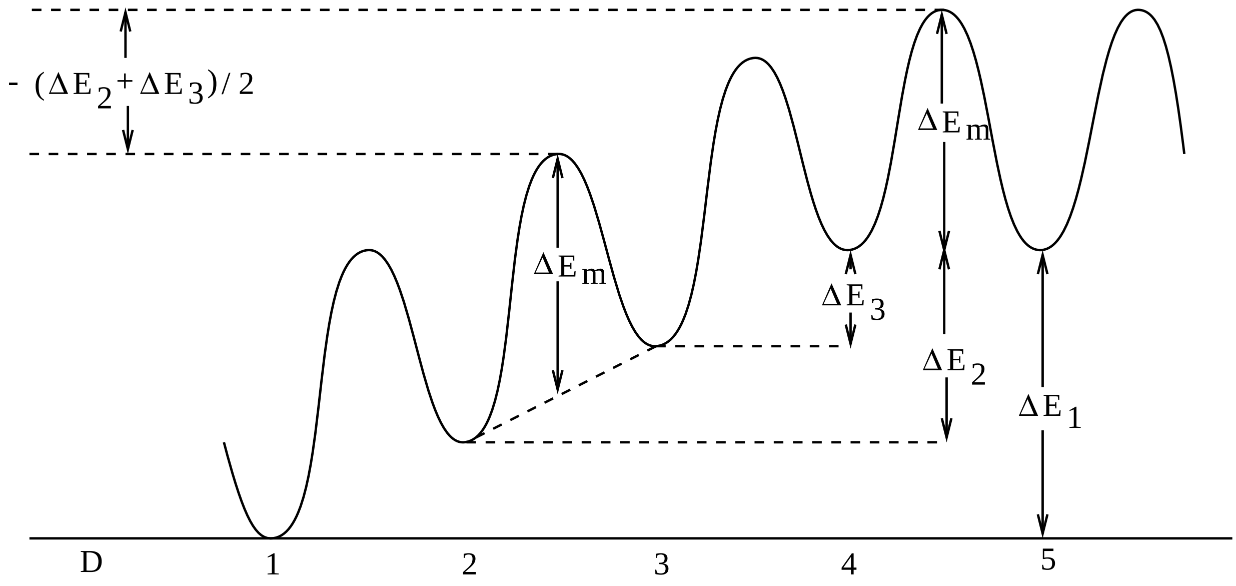

Figure 2: Schematic of vacancy energy as a function of position in the neighborhood of a dopant.

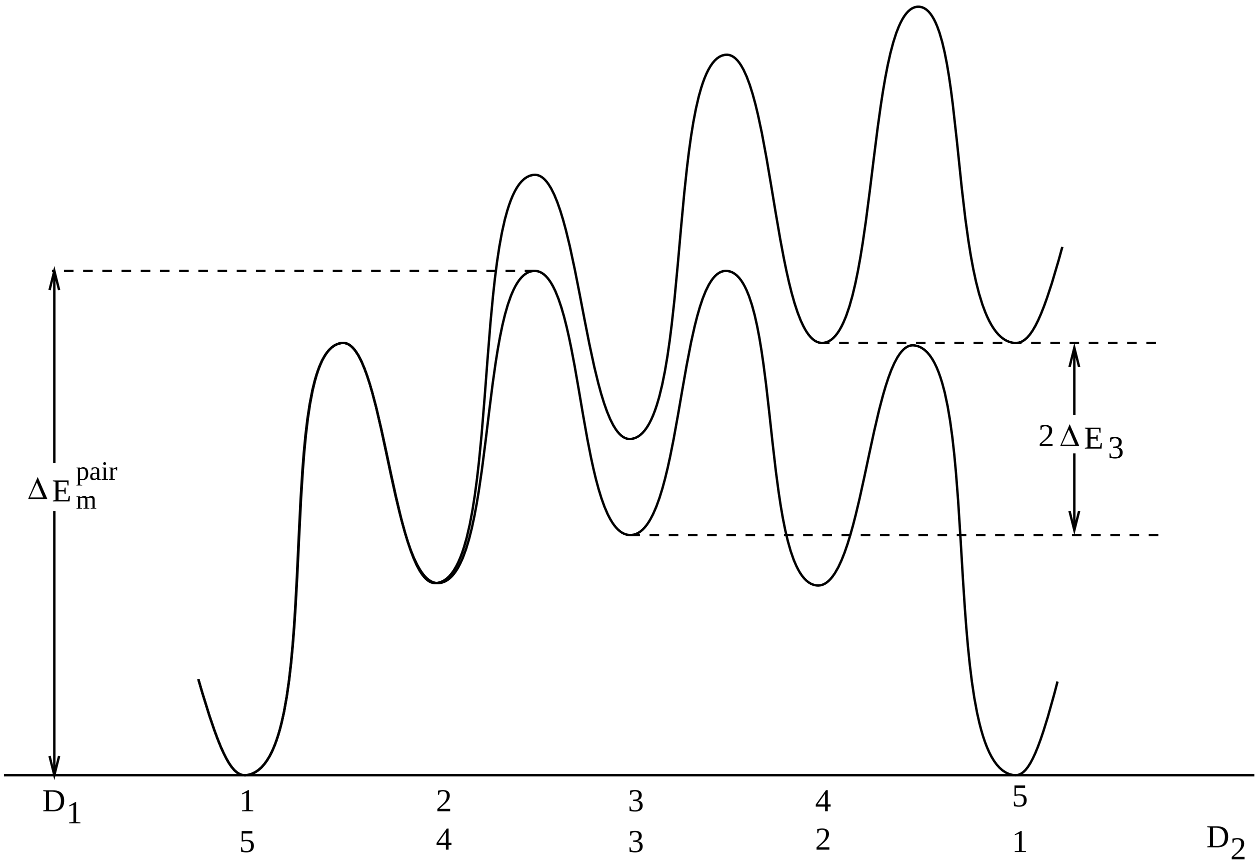

Figure 3: Comparison of vacancy energy as a function of position in the neighborhood of one versus two dopant atoms.

[5] S. M. Hu, *Phys. Stat. Sol. B* **60**, 595 (1973).

[6] A. D. Le Claire and A. B. Lidiard, *Philos. Mag.* **1**, 518 (1956).

[7] K. Compaan and Y. Haven, *Trans. Faraday Soc.* **54**, 1498 (1958).

[8] D. Mathiot and J. C. Pfister, *J. Phys. Lett.* **43**, L-453 (1982).

[9] D. Mathiot and J. C. Pfister, *J. Appl. Phys.* **66**, 1970 (1989).

[10] M. Hirata, M. Hirata and H. Saito, *J. Phys. Soc. Jap.* **27**, 405 (1969).

[11] B. J. Masters and J. M. Fairfield, *J. Appl. Phys.* **40**, 2390 (1969).

[12] R. B. Fair in **Impurity Doping Processes in Silicon**, ed. F. F. Y. Yang (North-Holland, New York, 1981) p. 315.

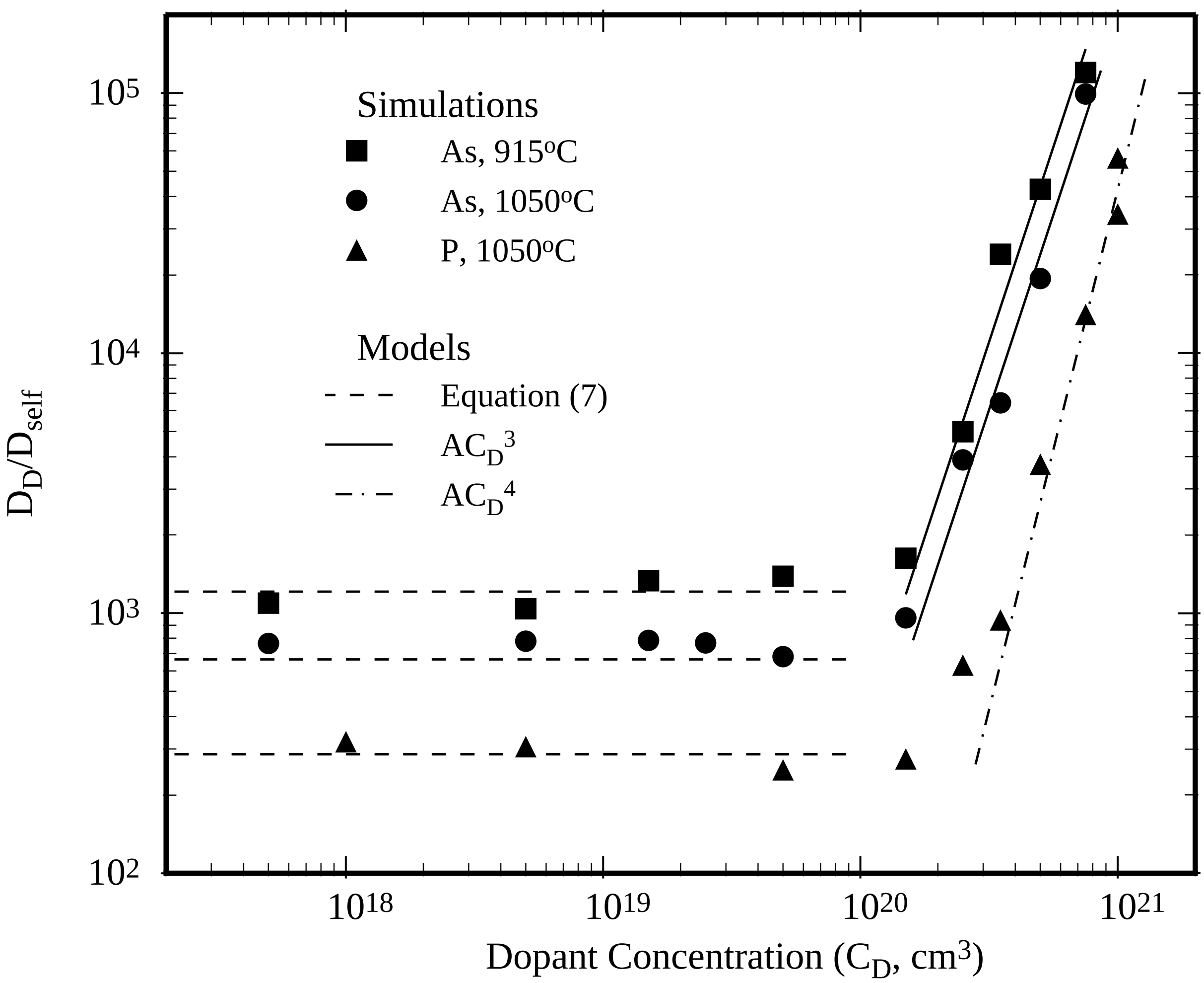

Figure 4: Normalized diffusivity versus doping density at 915 and 1050°C using the pair binding energy for arsenic and at 1050°C using the pair binding energy of phosphorus [10]. At high concentrations, the normalized diffusivity is approximately proportional to C_D^n with $3 < n < 4$ as indicated. Also shown for comparison is the analytic predictions for diffusivity in moderately doped material (Equation 7, dashed lines).

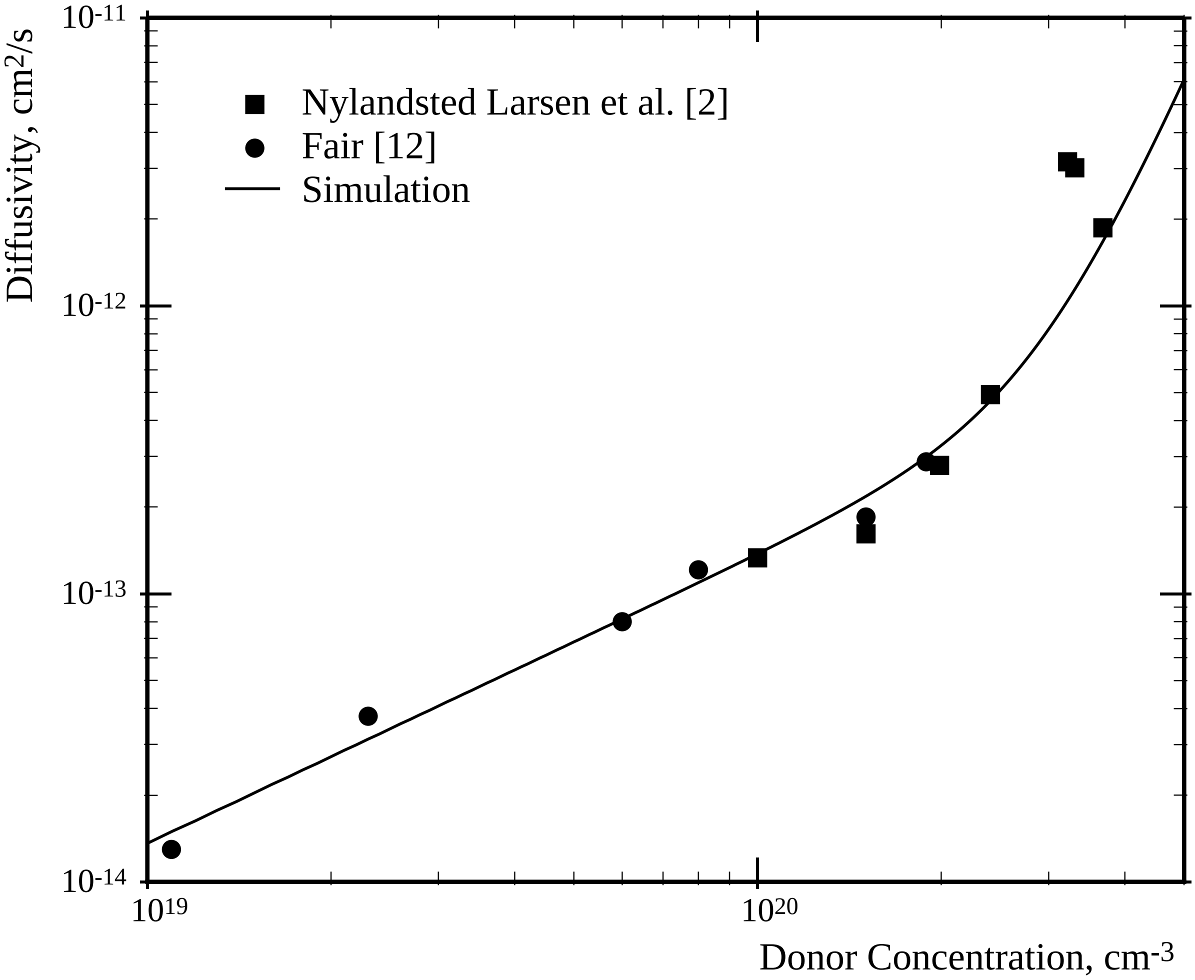

Figure 5: Comparison of experimental measurement of arsenic diffusivity at 1050°C versus doping level to lattice Monte-Carlo simulations. The diffusivity for moderate doping levels is fit assuming diffusion via negatively-charged vacancies and then extrapolated to higher doping levels using the simulation results.